Numerical Analysis of Marangoni Convection in Bridgman Method

By

Hiroyuki UCHIDA*, Keiichi KUWAHARA* and Shintaro ENYA*

(February 5, 1987)

1. INTRODUCTION

It is expected to obtain high quality crystal in the material processing in space, because the buoyancy driven natural convection diminishes under microgravity condition. Under such condition, free convection driven by the surface tension, so-called Marangoni convection, becomes usually dominant. In order to estimate the quality of products and to design the material processing facility, investigation on the Marangoni convection is essential.

In these years, Kuwahara, Maekawa, *et al.* [1–4] have been studying Marangoni convection both experimentally and numerically related to crystal growth techniques in space. Bergman, *et al.* [5], Srinivasan, *et al.* [6] and Bauer, *et al.* [7] also analyzed Marangoni convection under various situations. In the present study, Marangoni convection in Bridgman method is analyzed, which is one of crystal growth methods. After brief description for mathematical formulation, discussion will be made for flow field and heat transfer.

2. GOVERNING EQUATIONS AND NUMERICAL METHOD

We consider two-dimensional steady incompressible laminar flow and heat transfer in the present study. Governing equations are given as

$$\rho\frac{\partial u_i}{\partial t}+\rho u_j\frac{\partial u_i}{\partial x_j}=-\frac{\partial p}{\partial x_i}+\mu\frac{\partial^2 u_i}{\partial x_j\partial x_j}+\rho g_i\beta(T-T_m) \tag{1}$$

$$\frac{\partial u_j}{\partial x_j}=0 \tag{2}$$

$$\frac{\partial T}{\partial t}+u_j\frac{\partial T}{\partial x_j}=a\frac{\partial^2 T}{\partial x_j\partial x_j} \tag{3}$$

Equations (1) through (3) express the conservation of momentum, mass and energy. These equations are described by using the Einstein convention of summing over a

* Research Institute, Ishikawajima-Harima Heavy Industries Co., Ltd.

repeated subscript. In these equations, x_i, u_i are the Cartesian coordinates and the velocity components in the ith coordinates, and p the pressure, T the temperature, ρ the density, μ the viscosity, g the gravitational acceleration, β the coefficient of volume expansion, a the thermal diffusivity, T_m the mean temperature. In the transport equations (1) and (3), t denotes the fictitious time introduced in order to obtain steady solution by using the time-marching method. The first term of right hand side of Eq. (1) is neglected since pressure will not be dominant in the present flow problem.

Nondimensional forms of Eqs. (1) through (3) are obtained as

$$\frac{\partial U_i}{\partial \tau}+U_j\frac{\partial U_i}{\partial X_j}=\frac{\partial^2 U_i}{\partial X_j \partial X_j}+Gr(\theta-\theta_m) \tag{4}$$

$$\frac{\partial U_j}{\partial x_j}=0 \tag{5}$$

$$\frac{\partial \theta}{\partial \tau}+U_j\frac{\partial \theta}{\partial X_j}=Pr^{-1}\frac{\partial^2 \theta}{\partial X_j \partial X_j} \tag{6}$$

where the nondimensional variables are defined by

$$\begin{aligned} &X_i=x_i/L, \qquad \tau=t\nu/L^2 \\ &U_i=u_i/u_0, \qquad u_0=\nu/L \\ &\theta=(T-T_c)/(T_h-T_c) \end{aligned} \tag{7}$$

in which L is the characteristic length, u_0 is the reference velocity, $\nu=\mu/\rho$ is the kinematic viscosity, and the subscripts h and c express the values at hot and cold wall. Equations (4) and (6) are characterized by two nondimensional numbers:

$$Gr=g\beta(T_h-T_c)L^3/\nu^2 \qquad \text{(Grashof number)} \tag{8}$$

and

$$Pr=\nu/a \qquad \text{(Prandtl number)} \tag{9}$$

In the present study, boundary conditions are specified on a hot wall, a cold wall, a stationary thermally insulated boundary, a symmetry boundary and a free surface. On the hot wall and the cold wall, the normalized temperature is fixed to unity and zero, respectively, and the velocity components are set to zero there. On the other boundaries, the temperature gradient normal to the boundaries are set to zero. On the stationary boundary, the velocity components are set to zero. On the symmetry boundary, normal component of the velocity is set to zero, and gradient of tangential component of the velocity is set to zero.

Since the surface tension balances with the shear stress on the free surface, following equation is coupled with a momentum transport equation.

$$\mu\frac{\partial u}{\partial y}=-\sigma_t\frac{\partial T}{\partial x} \tag{10}$$

is which σ_t is the temperature coefficient of surface tension σ:

$$-\sigma_t=\frac{\partial\sigma}{\partial T} \tag{11}$$

Nondimensional form of Eq. (10) can be obtained as

$$\frac{\partial U}{\partial Y}=-\frac{Ma}{Pr}\cdot\frac{\partial\theta}{\partial X} \tag{12}$$

in which Ma is the Marangoni number defined by

$$Ma=\sigma_t L(T_h-T_c)/\mu a \tag{13}$$

This Marangoni number plays a main role in the surface tension driven natural convection.

In order to solve those nondimensional transport equations (4) and (6), time-marching method is employed. These equations are discretized in space and time by using the finite difference method. Centered space difference formulae for uniform mesh and leap-frog scheme [8] are employed. Velocity correction method [9], so-called SMAC method, is adopted to combine the equation of continuity with the equations of motion.

3. Numerical Results and Discussion

At first, a preparative computation was carried out in order to test the applicability of the present numerical method to the analysis of the Marangoni convection.

Figure 1 shows the present results of the temperature and velocity distribution. They are compared with Ochiai's experimental and numerical result [2]. Boundary conditions of this problem is as follows: the right and the left boundary are hot and cold wall. The lower and the upper boundary are adiabatic wall and free surface. The gravity force is considered in this analysis in order to compare with Ochiai's experimental result obtained on earth. Marangoni number and Rayleigh number are 35 and 120, respectively, where the distance between cold and hot wall is used as the reference length. Silicone oil, of which Prandtl number is 9,200, is considered.

The temperature distribution is shown in Fig. 1 (a) by means of isothermal lines. The present result shows very good agreements with Ochiai's numerical result [2]. The velocity distribution is shown in Fig. 1 (b) by means of streamlines. The present result shows a good agreement with Ochiai's result about the location of vortex center and overall flow pattern. But the streamlines themselves does not seem to agree well, probably because the plotting interval of stream function used for the present result is

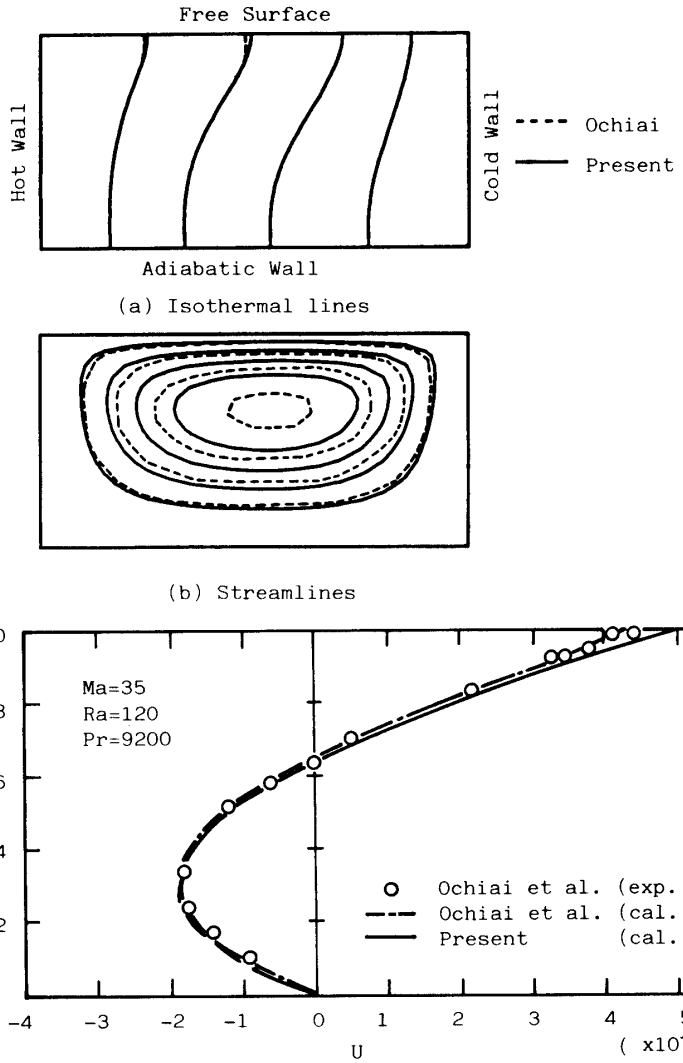

Fig.1(c) Velocity distributions on center vertical plane.

Fig. 1. Marangoni convection solution of preparative analysis.

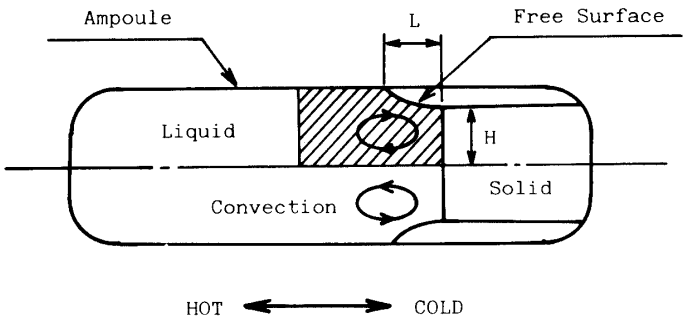

Fig. 2. Concept of Bridgman crystal growth method.

different from Ochiai's one. Furthermore, the velocity distributions on the center vertical plane are shown in Fig. 1 (c). The present result shows good agreements with both numerical and experimental results [2]. It can be concluded for this preparative

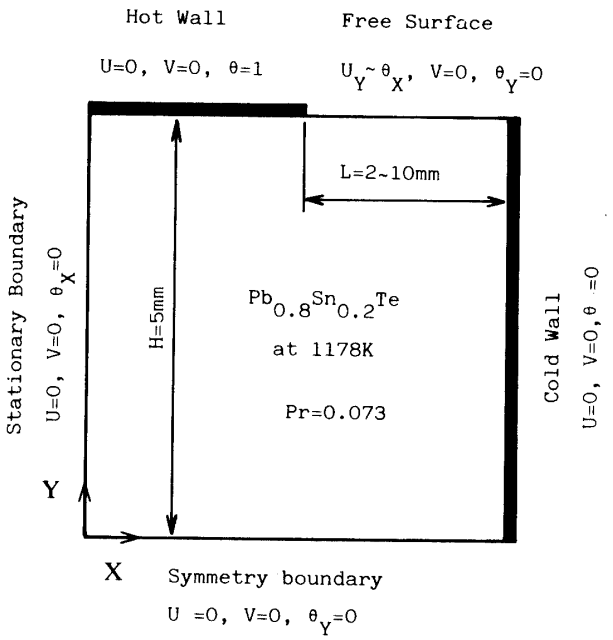

Fig. 3. Boundary conditions for analysis of Marangoni convection in Bridgman method.

analysis that the present numerical method is valid to predict the Marangoni convection.

Next to the preparative analysis, Marangoni convection in Bridgman method was analyzed. The concept of crystal growth by the Bridgman method is schematically shown in Fig. 2. The molten material which fills the ampoule is chilled from one side, then the material is solidified gradually. A vacant space will be formed in the ampoule due to the contraction of the material. Consequently, a free surface of liquid is formed, and a free convection as shown in Fig. 2 will appear. A purpose of this analysis is to investigate the influences of the length of free surface and the temperature difference between two heat transfer walls upon the fluid flow and the heat transfer. A shaded part in this figure shows the computation domain which was approximately treated by using the Cartesian coordinates.

A rectangular computation domain is considered as shown in Fig. 3. A left half and a right half of the upper boundary are the hot wall and the free surface, respectively, and the right boundary is the cold wall. The height H of the cold wall was fixed to be 5 mm. The length L of the free surface was given to be 2, 5 or 10 mm. The temperature difference T_h-T_c was given to be 2, 5 or 10 K. Thermal properties of PbSnTe at 1,178 K were used. The left and the lower boundary are stationary and symmetry boundary.

Figure 4 shows the streamlines for L=2, 5 and 10 mm. Marangoni numbers based on L are 212, 530 and 1,060 for each case. These flow patterns are characterized by the location of the vortex center. In the case of small L, vortex center is located near free surface. Influence of the convection is limited near the free surface. In the case of large L, the vortex center approaches to middle plane between free surface and symmetry boundary. In the near region of the hot wall, convective heat transfer does

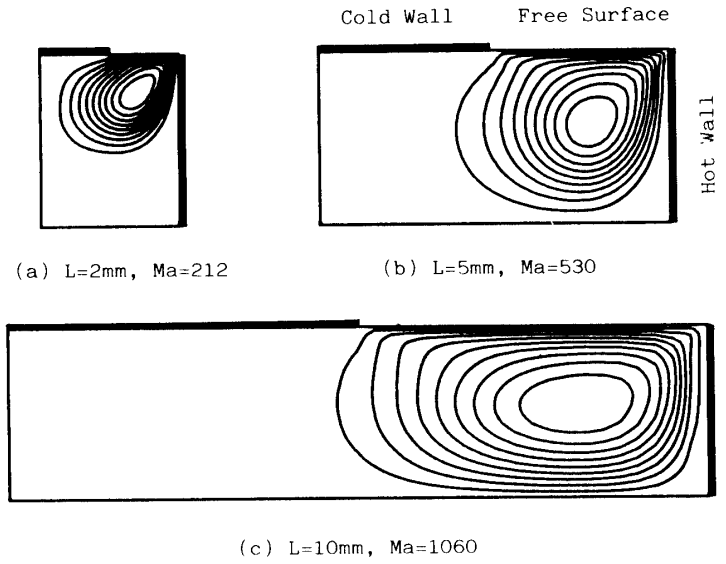

Fig. 4. Streamlines of Marangoni convection in Bridgman method.

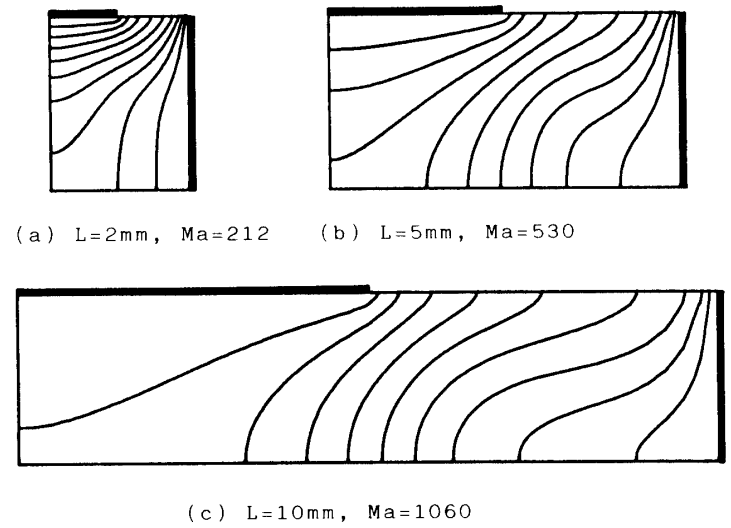

Fig. 5. Isotherms of Marangoni convection in Bridgman method.

not seem to be dominant in each case, because the velocity is very small there. Figure 5 shows the temperature distributions corresponding to Fig. 4.

Furthermore, the heat transfer on the cold wall was studied. The cold wall is the simple model of the solidification surface, which plays an important role in the crystal growth. Nondimensionalized heat transfer coefficient, i.e., the Nusselt number, is defined by

$$Nu = hL/\lambda \tag{14}$$

where h is the heat transfer coefficient, λ the thermal conductivity. By integrating the distribution of the local Nusselt number along the cold wall, average Nusselt number is obtained as

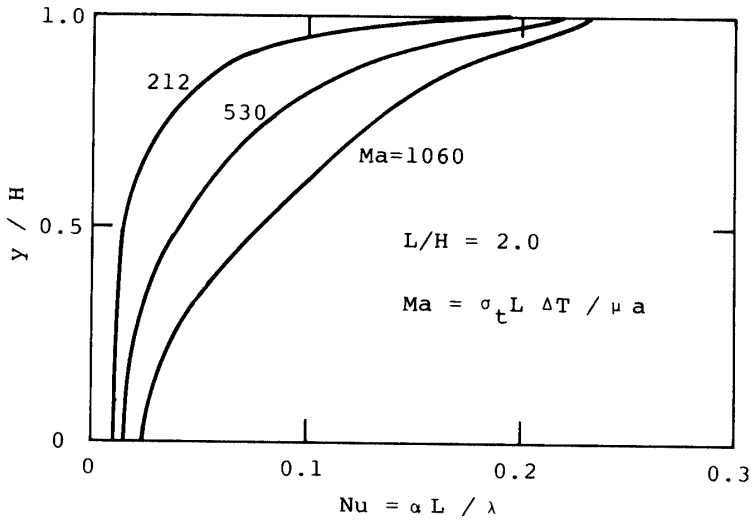

Fig. 6. Local Nusselt number distribution on cold wall.

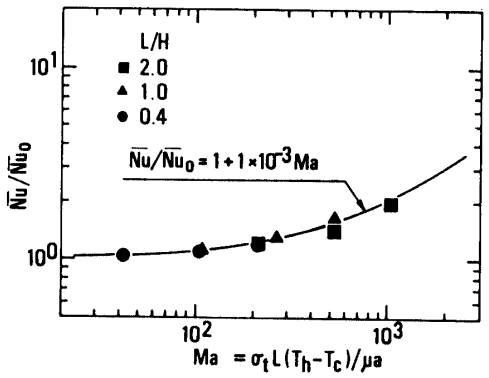

Fig. 7. Average Nusselt number vs. Marangoni number.

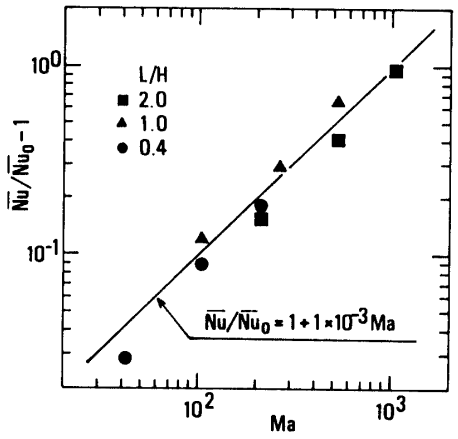

Fig. 8. Average Nusselt number (net convective heat transfer) vs. Marangoni number.

$$\overline{Nu}=\int_0^H Nu\,dy/H \tag{15}$$

In the following discussion, another Nusselt number $\overline{Nu}_0$ will be employed. It is previously obtained from heat conduction analysis in which the convective heat transfer is neglected.

Figure 6 shows an example of the distribution of local Nusselt number on the cold wall. These distributions deviate upward, and they are spread as the Marangoni number increases. This is able to understand from that the influence of the flow field on the heat transfer is spread from free surface as the Marangoni number increases.

Figure 7 shows the correlation between the average Nusselt number and the Marangoni number. In this analysis, two nondimensional numbers, i.e., the Marangoni number *Ma* and the aspect ratio *L/H*, are the governing parameters. The normalized Nusselt number $\overline{Nu}/\overline{Nu}_0$ approaches to unity as the Marangoni number

decreases. Nine data are obtained by changing the length of the free surface and the temperature difference. The data are distributed close to a curve. An approximate formula of this curve is obtained from Fig. 8 as

$$\overline{Nu}/\overline{Nu}_0 = 1 + 1 \times 10^{-3} Ma \tag{16}$$

Therefore, the heat transfer is only governed by Marangoni number within the range of the parameters given in the present analysis. The influence of the aspect ratio does not seem to be significant. The ordinate of Fig. 8 expresses a ratio of the net convective heat transfer rate to the conductive one. The linear correlation, expressed by Eq. (16), can be obtained.

These computations were carried out on a personal computer NEC PC-98XA with a fast floating-point processor. It took about two or three hours for each run. By using the 41×21 grid points, converged solutions were typically obtained after 600 time steps for $\varepsilon < 10^{-4}$, where ε is a criterion for the relative error of the nondimensional temperature.

4. Conclusion

Natural convection driven by the surface tension, so-called Marangoni convection, was analyzed by using the finite difference method. The result of the preparative computation was compared with Ochiai's experimental and numerical results [2]. They showed fairly good agreements. Further analysis was made for the mathematical model of Bridgman method. It was shown that the vortex center moves from near free surface toward the opposite boundary as the Marangoni number increases. A simple correlation between heat transfer coefficient and Marangoni number was also shown.

The present authors would like to express our sincere gratitude to Dr. Mikio Morioka of Ishikawajima-Harima Heavy Industries Co., Ltd. for his helpful advices on the arrangement of the data.

References

[1] K. Kuwahara, M. Morioka, J. Ochiai and S. Enya: "Fundamental Study of Marangoni Convection in Bridgman Method", Proceedings of the 15th International Symposium on Space Technology and Science, Tokyo, pp. 2161–2166 (1986).

[2] J. Ochiai, K. Kuwahara, M. Morioka, S. Enya, K. Sezaki, T. Maekawa and I. Tanasawa: "Experimental Study on Marangoni Convection", Proceeding of the 5th European Symposium on Material Sciences under Microgravity, pp. 291–295 (1984).

[3] K. Sezaki, S. Enya, M. Morioka, J. Ochiai, I. Tanasawa and T. Maekawa: "Two-Dimensional Convection in Liquid Layer Related to Crystal Growth Techniques in Space", Adv. Space Res., Vol. 3, No. 5, pp. 85–88 (1983).

[4] T. Maekawa, I. Tanasawa, J. Ochiai, K. Kuwahara, M. Morioka and S. Enya: "Two-Dimensional Marangoni and Buoyancy Convection Related to Crystal Growth Techniques in Space", Adv. Space Res., Vol. 4, No. 5, pp. 63–66 (1984).

[5] T. L. Bergman and S. Ramadhyani: "Combined Buoyancy- and Thermo-capillary Driven Convection in Open Square Cavities", Numerical Heat Transfer, Vol. 9, pp. 441–451 (1986).

[6] J. Srinivasan and B. Basu: "A Numerical Study of Thermocapillary Flow in a Rectangular Cavity during Laser Melting", Int. J. Heat Mass Transfer, Vol. 29, No. 4, pp. 563–572 (1986).
[7] H. F. Bauer: "Heat Transport in a Liquid Column in Weightless Conditions due to Thermal Marangoni", Numerical Heat Transfer, Vol. 8, pp. 81–97 (1985).
[8] Patrick J. Roache: "Computational Fluid Dynamics", Hermosa Publishers Inc. (1976).
[9] G. E. Schneider and G. D. Raithby: "Finite Element Analysis of Incompressible Fluid Flow Incorporating Equal Order Pressure and Velocity Interpolation", Computer Methods in Fluids, Pentech Press, London, pp. 49–83 (1980).